Inhibition of STAT3 Signaling Pathway by Nitidine Chloride Suppressed the Angiogenesis and Growth of Human Gastric Cancer

Jing Chen[1,2], Jieqiong Wang[1], Lei Lin[1], Lijun He[1], Yuanyuan Wu[1], Li Zhang[1], Zhengfang Yi[1], Yihua Chen[1], Xiufeng Pang[1,*], Mingyao Liu[1,3,*]

[1] Institute of Biomedical Sciences and School of Life Sciences, East China Normal University, Shanghai 200241, China; [2] Key Laboratory of Reproduction and Genetics in Ningxia, Ningxia Medical University, Yinchuan 750004, China; [3] Institute of Biosciences and Technology, Department of Molecular and Cellular Medicine, Texas A&M University Health Science Center, Houston, Texas 77030, USA.

Running title: Nitidine chloride suppresses tumor angiogenesis and growth

Key words: Nitidine chloride, angiogenesis, tumor growth, gastric cancer, STAT3

Financial support: This work is supported by the grants from National Natural Science Foundation of China (81101683 and 30930055), Chenguang Program from Shanghai Municipal Education Commission (10CG25), a grant from National Institute of Health (1R01 CA134731), and Fundamental Research Funds for the Central Universities (78210021).

***To whom correspondence should be addressed:**

Drs. Mingyao Liu or Xiufeng Pang

The Institute of Biomedical Sciences and School of Life Sciences, East China Normal University, 500 Dongchuan Road, Shanghai 200241, China. **Phone:** +86-21-54345016; **Fax:** +86-21-54344922; **E-mail:** myliu@bio.ecnu.edu.cn; xfpang@bio.ecnu.edu.cn

Disclosure Statement: No potential conflicts of interest were disclosed.

Abstract

Signal transducer and activator of transcription factor 3, STAT3, has been strongly implicated in human malignancies, and constitutive activation of STAT3 serves a crucial role in cell survival, angiogenesis, immune evasion and inflammation. In this study, we showed that nitidine chloride, a natural phytochemical alkaloid derived from *Zanthoxylum nitidum (Roxb) DC*, exerts potent anticancer activity through STAT3 signaling cascade. Nitidine chloride dose-dependently suppressed vascular endothelial growth factor (VEGF)-induced endothelial cell proliferation, migration and tubular-structure formation *in vitro*, and dramatically reduced VEGF-triggered neovascularization in mouse cornea and Matrigel plugs *in vivo*. This angiogenesis inhibition mediated by nitidine chloride was well interpreted by the suppression of Janus kinase 2/STAT3 signaling and STAT3 DNA-binding activity in endothelial cells. Furthermore, nitidine chloride suppressed the constitutively activated STAT3 protein, its DNA-binding activity, and the expression of STAT3-dependent target genes, including Cyclin D1, Bcl-xL and VEGF in human gastric cancer cells. Consistent with the above findings, nitidine chloride inhibited gastric tumor cell growth and induced tumor cell apoptosis *in vitro*, and effectively suppressed the volume, weight and microvessel density of human SGC-7901 gastric solid tumors (n=8) at a dosage of 7 mg/kg/d (intra-peritoneal injection). Immunohistochemistry and Western blot analysis further revealed that the expression of STAT3, CD31 and VEGF protein in xenografts was remarkably decreased by the alkaloid. Taken together, we propose that nitidine chloride is a promising anticancer drug candidate as a potent STAT3 signaling inhibitor.

Introduction

Gastric cancer is one of the most common digestive malignancies in the world (1). Despite considerable improvements achieved through systemic therapy, the treatment of gastric cancer especially remains extremely unfavorable, with a 5-year survival rate of only 10 to 15% (2). Limited effects of conventional chemotherapy drugs including capecitabine, 5-fluorouracil and paclitaxel on patient survival rate underscores the need for new strategies to inhibit gastric cancer growth. Gastric tumors can trigger substantial development of new blood vessels in a process called angiogenesis to nourish tumor growth (3). Angiogenesis is a rate-limiting process including the destabilization of integrated blood vessel, endothelial cell proliferation, migration and tubulogenesis. Numerous reports have shown that disrupting tumor angiogenesis effectively suppresses tumor growth and metastasis (4). As a potential target, the signal transducers and activators of transcription 3 (STAT3), has been shown to be highly expressed in gastric cancer and be strongly linked to tumor angiogenesis and metastasis (5). Therefore, searching for novel STAT3-targeted anti-angigogenic agents is urgently needed for all cancer treatments, including gastric cancer.

STAT3, a latent self-signaling transcription factor, is activated by certain interleukins (e.g., IL-6) and growth factors. Constitutive and aberrant activation of STAT3 occurs at a frequency of 50~90% in a broad range of human malignancies, suggesting that STAT3 pathway is significantly associated with tumor VEGF overproduction (6). Furthermore, recent studies have identified STAT3 as a direct transcriptional activator of VEGF and HIF-1α under hypoxia (7), which are key stimuli known to initiate endothelial cell migration, and differentiation. Upon activation, STAT3 undergoes phosphorylation, homodimerization, nuclear translocation, and DNA binding, which subsequently

leads to transcription of various target genes, such as Cyclin D1, Bcl-2, Bcl-xL, MMP2 and VEGF, to regulate cell survival, angiogenesis, immune evasion and inflammation in tumor microenvironment (8-10). Interfering with activated STAT3 signaling contributes to angiogenesis inhibition, tumor growth arrest and metastasis suppression (11-12). Currently, STAT3 inhibitor, including natural compounds, peptide, peptidomimetic compounds, small molecules and oligonucleotides, have been developed and are undergoing into clinical settings (4, 13,14). Thus, agents that suppress STAT3 activation are promising for prevention and treatment of cancer.

Nitidine chloride (Fig. 1A), a natural bioactive phytochemical alkaloid derived from *Zanthoxylum nitidum (Roxb) DC,* was initially reported to have significant antioxidant, antifungal, anti-inflammatory and analgesic bioactivities (15). Subsequent studies proved that nitidine chloride exhibited anticancer potential through the induction of apoptosis in a wide variety of human tumor cell lines, such as lung, breast, liver, oral and osteosarcoma *in vitro* (16). Activation of caspase-3 (17), inhibition of topoisomerase I (18), and suppression of human immunodeficiency virus reverse transcriptase (19) have been implicated in niditine-mediated anticancer and immunomodulatory function. However, the precise molecular target and underlying mechanisms of its antitumor efficacy are poorly defined to date.

Considering the critical roles of STAT3 signaling in the angiogenic and neoplastic process (20-21), we screened a number of natural compounds and found that nitidine chloride exerted its anti-angiogenic and anti-tumor property through the suppression of STAT3 pathway. We provide evidence that nitidine chloride dose-dependently suppresses the activation of STAT3, its

DNA-binding activity and its transcriptional activity in both human endothelial cells and gastric cancer cells. As a result, nitidine chloride effectively inhibited tumor angiogenesis and tumor growth in an experimental gastric cancer xenograft mouse model. Therefore, our findings indicate that nitidine chloride is a promising candidate compound that can be further optimized to be a therapeutic agent for gastric cancer.

Materials and Methods

Reagents. Nitidine chloride (purity > 98%) was purchased from Shanghai Winherb Medical Science (Shanghai, China). A 50 mmol/L stock solution was prepared in dimethyl sulfoxide (DMSO) (Sigma, St. Louis, MO), stored at -20°C and then diluted as needed in cell culture medium. Recombinant human VEGF ($VEGF_{165}$) was a gift from the Experimental Branch of the National Institutes of Health (NIH; Bethesda, MD). Growth factor-reduced Matrigel was obtained from BD Biosciences (San Diego, CA). Most appropriate antibodies were purchased from Cell Signaling Technology (Danvers, MA), unless otherwise specified.

Cell culture. Primary human umbilical vascular endothelial cells (HUVECs) were a gift from Dr. Xinli Wang (Cardiothoracic Surgery Division of Michael E. DeBakey Department of Surgery, Baylor College of Medicine, Houston, TX) and cultured in endothelial cell culture medium (ECM) as described previously (22). HUVECs were confirmed by their typical microscopic morphology: homogeneous, large, polygonal and cobblestone-like. Human gastric cancer AGS cells were purchased from American Type Culture Collection (Manassas, VA), and SGC-7901, MGC-803, BGC-823 cancer cell lines were obtained from the China Center for Type Culture Collection (Shanghai, China). Gastric cancer cells were cultured in RPMI 1640 medium supplemented with 10% fetal bovine serum (HyClone Laboratories, Logan, UT). All the above cells were maintained at 37°C in a humidified incubator containing 5% CO_2.

Cell viability assay. Briefly, HUVECs ($3\sim4\times10^4$ cells/well) were seeded in 96-well plates, exposed to various concentrations of nitidine chloride and with VEGF (50 ng/mL) for 48 h. Those gastric

cancer cells (6×10^3 cells/well) were directly treated with nitidine chloride (5, 10, 20, 40, 60 μmol/L) for consecutive 48 h measured by MTS assay (22). Three independent experiments with triplicate were performed.

Endothelial cell migration assay. To determine the effect of nitidine chloride on HUVECs motility *in vitro*, we performed cell migration assay using gelatin-coat Boyden inserts (8-μm) (BD Biosciences). Serum-starved HUVECs ($4\sim6\times10^4$ cells) in 100 μL ECM containing 0.5% FBS were pretreated with nitidine chloride (0.5, 1, 5, 10 μmol/L) for 30 min. Those cells were then seeded on the upper chamber of Transwell and allowed to migrate to the lower chamber with 500 μL ECM containing 0.5% FBS and 50 ng/mL VEGF. After 5~7 h incubation, non-migrated cells were removed with cotton swabs, and migrated cells were fixed with cold 4% paraformaldehyde and stained with 1% crystal violet. Images were taken using an inverted microscope (Olympus; magnification, 100×), and migrated cells in random four fields were quantified by manual counting. Three independent experiments with triplicate were performed.

Endothelial cell capillary-like tube formation assay. Formation of tubular structures of endothelial cell was studied *in vitro* as previously described (23). HUVECs were pretreated with nitidine chloride (5, 10 μmol/L) for 1 h and then seeded onto the Matrigel layer in 48-well plates at a density of $5\times10^4\sim1\times10^5$ cells/well. After incubation for 6~8 h, angiogenesis was assessed based on formation of capillary-like structures. Tubes in randomly chosen microscopic fields were photographed (Olympus; original magnification, 100×). Three independent experiments were performed.

Animal studies. C57BL/6 and nude mice used in our present study were purchased from National Rodent Laboratory Animal Resources (Shanghai, China) and maintained according to the NIH standards established in the "Guidelines for the Care and Use of Experimental Animals". All of the experimental protocols were approved by the Animal Investigation Committee of East China Normal University.

Matrigel plug assay. As described elsewhere (24), 0.5 mL of Matrigel in the presence or absence of 100 ng VEGF and 20 units of heparin, plus indicated amount of nitidine chloride (30, 60 μg) was subcutaneously injected into the ventral area of C57/BL/6 mice (n=4~6). Seven days after the implantation, intact matrigel plugs were carefully removed. Those plugs were then fixed and embedded in paraffin. Specific blood vessel staining with CD31 antibody was performed on the 5-μm sections according to the protocol. Microphotographs were taken by Leica DM 4000B photomicroscope (Solms, Germany; magnification, 400×).

Mouse corneal micropocket assay. The modified mouse cornea micropocket angiogenesis assay was performed as previously described (25). Micropellets were made of sucrose aluminum sulfate and Hydron pellets (polyhydroxyethyl-methacrylate), containing VEGF (100 ng) with or without nitidine chloride (15 μg/pellet). Seven days later, eyes were photographed. Maximal vessel length and clock hours of circumferential neovascularization were measured by the Image-Pro plus 6.0 software package (Media Cybernetics Inc., Bethesda, MD) and vessel area was calculated according to the formula of $0.2\pi \times \text{length} \times \text{clock number}$. Two independent experiments were performed.

Live/dead staining assay. Apoptosis of cells was also determined by live/dead reagent (Invitrogen, Carlsbad, CA), which was used to measure intracellular esterase activity and plasma membrane integrity (26).

Annexin V/propidium iodide staining assay. Nitidine chloride-mediated cell apoptosis was assayed by annexin V-FITC and propidium iodide staining (ApopNexin Annexin V FITC apoptosis kit; Millipore) as described earlier (23).

Immunofluorescence assay. Briefly, SGC-7901 (6×10^4 cells) were treated with nitidine chloride (30 μmol/L) for phosphorylation of STAT3 (Tyr^{705}) detection in the nuclei using immunofluorescence analysis (27). The images were captured by confocal laser scanning microscopy (LSM 5 PASCAL; Carl Zeiss, Germany; magnification, 600×).

Western blotting analysis. HUVECs were first starved in serum-free ECM for 4~6 h and then pretreated with nitidine chloride, followed by the stimulation with 50 ng/mL of VEGF for 2~20 min. Tumor cells were directly exposed to nitidine chloride. The whole cell extracts were prepared by lysis buffer supplement with different kinds of protein inhibitors. Equal protein aliquot of each lysate was subjected to SDS-PAGE (6%~12%), blotted onto PVDF membrane (Bio-Rad, Hercules, CA), probed with specific antibodies and subsequently detected by chemiluminescence. Protein concentration was determined using Micro BCA™ Protein Assay Kit (Pierce Biotechnology, Rockford, IL).

RNA isolation and reverse transcription polymerase chain reaction (RT-PCR). Total RNA from SGC-7901 cancer cells treated with nitidine chloride (30 μmol/L) for different intervals was extracted using the Trizol reagent and converted to cDNA by RT-PCR kit (Invitrogen, Carlsbad, CA). GAPDH was used as loading control.

Electrophoretic mobility shift assay (EMSA). DNA binding activity of STAT3 was examined by electrophoretic mobility shift assay using IRDye700 infrared Dye Labeled oligonucleotide probe (LI-COR, Bio-sciences, US) and analyzed in both HUVECS and SGC-7901 cells based on conditions defined previously(28).

Chromatin immunoprecipitation assay. SGC-7901 cells were treated with various concentrations (10, 20, 40 μmol/L) of nitidine chloride for 48 h, fixed with 1% formaldehyde and lysed as described previously(29). Chromatin samples were immunoprecipitated with antibodies against STAT3 or with normal rabbit IgG antibody, and examined by quantitative PCR using the SYBR Premix Ex Taq Kit (TaKaRa Biotechnology, Shanghai, China).

Human gastric tumor xenograft mouse model. Briefly, SGC-7901 cancer cells (4×10^6 cells/mouse) were injected subcutaneously into the right flank of 6-week-old male BALB/cA nude mice (National Rodent Laboratory Animal Resources, Shanghai, China). After tumor grew to about 70 mm^3, the mice were randomly assigned into two groups (n=8), and treated with or without nitidine chloride (7 mg/kg/d) via intraperitoneal injection for consecutive 20 d. The mice of control group were administrated with same amount of DMSO. At the same time, solid tumor volume was determined

using Vernier caliper measurements and the formula of $A \times B^2 \times 0.52$, where A is the longest diameter of the tumor and B is the shortest diameter of the tumor. After 20 d, solid tumors were harvested and analyzed for immunohistochemistry (Lifespan Biosciences, Seattle, WA) and Western blotting.

Histology and immunohistochemistry. Solid tumors were removed, fixed with 10% formaldehyde, and embedded in paraffin. Immunohistochemical staining for STAT3, VEGF and CD31 were performed. Images were taken using a Leica DM 4000B photo microscope (Solms, Germany; magnification, 400×).

Statistical analysis. Statistical comparisons between groups were performed using one-way analysis of variance followed by Dunnet's test. Data were presented as means ± standard deviations. P values ≤ 0.05 were considered statistically significant.

Results

Nitidine chloride inhibits VEGF-induced endothelial cell proliferation, migration and tubular-structure formation *in vitro*.

To systematically address the inhibitory activity of nitidine chloride on tumor angiogenesis, we first evaluated its antiangiogenic function *in vitro*. As shown in Fig.1B, nitidine chloride dose-dependently decreased VEGF-induced cell viability in HUVECs, with the half maximal inhibitory concentration (IC_{50}) of 5 μmol/L. Given the importance of vascular endothelial cell motility in the process of angiogenesis (30), we further evaluated the potential effect of nitidine chloride on endothelial cell migration. Results showed that treatment with nitidine chloride (5~10 μmol/L) remarkably impaired the chemotactic motility of HUVECs in Boyden chamber assays (Fig.1C). The invasive cell number of nitidine chloride-treated HUVECs was much less than that of the control group ($P < 0.01$).

To better characterize the inhibitory function of nitidine chloride on neovascularization, we performed two-dimensional Matrigel assays. As shown in Fig.1D, endothelial cells differentiate and spontaneously align to form a capillary-structure network on Matrigel layer (Control). Nitidine chloride at tested concentrations (>1 μmol/L) significantly suppressed or inhibited the tubular structure formation of endothelial cells (Fig. 1D).

Nitidine chloride inhibits VEGF-induced angiogenesis *in vivo*.

We further explored the anti-angiogenic activity of nitidine chloride using two *in vivo* angiogenesis models, the Matrigel plug assay and the mouse corneal micropocket assay. As showed in Fig. 2A, Matrigel plugs containing VEGF alone appeared dark red, indicating that functional

vasculatures had formed inside the Matrigel via angiogenesis triggered by VEGF. In contrast, the addition of different amounts of nitidine chloride (30 μg or 60 μg per plug) to the Matrigel plugs containing VEGF dramatically inhibited vascular formation (Fig. 2A). These plugs displayed much paler appearance at 30μg and showed almost no vascular formation at 60μg (Fig. 2A, bottom, VEGF+NC 60μg). Immunohistochemistry staining indicates that large amount of CD31-positive endothelial cells existed inside the VEGF alone plugs, whereas the number of CD31-positive endothelial cells in nitidine chloride-treated plugs had dramatically decreased (Fig. 2B).

We next confirmed the *in vivo* anti-angiogenic functions of nitidine chloride in the mouse corneal micropocket assay. As shown in Fig. 2C, VEGF (100 ng) could significantly induce neovascularization in mouse cornea. In contrast, treatment with nitidine chloride (15 μg/mouse) led to a predominant reduction of angiogenesis in corneal vessel area as indicated by vessel length, clock number and vessel area. These results indicated that nitidine chloride inhibited VEGF-induced angiogenesis *in vivo.*

Nitidine chloride blocks VEGF-induced STAT3 activation in endothelial cells.

To figure out the molecular basis of nitidine chloride in antiangiogenesis, we examined the signaling pathways mediated by nitidine chloride in HUVECs using Western blot analysis and EMSA. It has been known that VEGF signaling events relevant to tumor angiogenesis are mainly mediated by VEGF receptor 2 (VEGFR2) phosphorylation (23). Therefore, we first tested the action of nitidine chloride on this critical receptor-tyrosine-kinase on endothelial cell membrane. We found that 5 μmol/L of nitidine chloride significantly inhibited the phosphorylation of VEGFR2 at Tyr^{1175} site (Fig. 3A). Since VEGF can trigger the activation of STAT3 signaling in HUVECs, we examined

the effects of nitidine chloride on the phosphorylation of STAT3 and shown that nitidine chloride dose- (Fig. 3B1) and time- (Fig. 3B2) dependently suppressed the phosphorylation of STAT3 (Tyr^{705}), with the maximum inhibition at 5~10 μmol/L. When noted, such inhibitory action of nitidine chloride on STAT3 was in parallel with a rapid de-phosphorylation of upstream kinases of STAT3, including JAK1 ($Tyr^{1022/1023}$), JAK2 ($Tyr^{1007/1008}$) and c-Src (Tyr^{416}) (Fig. 3B).

STAT3 translocation to the nucleus results in a specific DNA binding that in turn regulates target gene transcription, we next determined whether nitidine chloride suppressed DNA-binding activity of STAT3 using EMSA assay. Our results showed that nitidine chloride decreased STAT3 DNA binding activity in a concentration-dependent manner (Fig. 3C). These results provide evidence that nitidine chloride blocked angiogenesis by targeting STAT3 signaling pathway.

Nitidine chloride suppresses STAT3 signaling in gastric cancer cells.

Our study demonstrated that nitidine chloride exerts antiangiogenic activity *in vitro and vivo* through blocking STAT3 pathway in endothelial cells, with effective concentrations around 10 μmol/L, suggesting that STAT3 is a potential target of nitidine chloride in gastric cancer cells. To address such a possibility, we examined the inhibitory effect of niditine chloride on STAT3 in two human gastric cancer cell lines, SGC-7901 and AGS, which are known to express constitutive-active STAT3 protein (31-32). As expected, nitidine chloride blocked STAT3 phosphorylation in SGC-7901 cancer cells in dose- and time- dependent manners in both whole-cell lysate (Fig. 4A) and the nuclear translocation assays (Supplemental fig. B). We similarly verified the effects of nitidine chloride on activity of STAT3 in AGS gastric cancer cells (Supplemental fig. A). Moreover, DNA binding ability of STAT3 was also remarkably inhibited by nitidine chloride, as indicated by EMSA

analysis (Fig. 4B), with an effective concentration of 20 μmol/L.

Nitidine chloride suppresses STAT3 transcriptional activity in gastric cancer cells.

STAT3 participates in oncogenesis through up-regulation of genes encoding apoptosis inhibitors (Bcl-xL, Bcl-2 and survivin), cell cycle regulators (Cyclin D1 and c-Myc), and inducers of angiogenesis (VEGF) (8). We next examined whether the expression of these STAT3 target genes is down-regulated by nitidine chloride in SGC-7901 cancer cells. Our results showed that both mRNA and protein levels of Cyclin D1, Bcl-2, Bcl-xL and VEGF were significantly decreased by the treatment of nitidine chloride, with maximum suppression observed at around 12 to 24 h (Fig. 4C). In agreement, *in vivo* binding of Bcl-xL, Cyclin D1 and VEGF to STAT3 was also dose-dependently inhibited by nitidine chloride analyzed by chromatin immunoprecipitation (Fig. 4D).

Nitidine chloride inhibits cell viability and induces apoptosis in gastric cancer cells.

Since nitidine chloride suppressed the activation of STAT3 and STAT3-regulated proliferative gene products, we speculated that this compound could block cancer cell growth. Results in Fig. 5A showed that nitidine chloride remarkably suppressed the viability of several gastric cancer cell lines, with an IC_{50} of about 20 μmol/L. In addition, we further investigated the pro-apoptotic effects of nitidine chloride using live-dead staining, flow cytometry, and Western blot assays. As shown in Fig.5B, nitidine chloride dose-dependently potentiated cancer cell death, with an IC_{50} at about 20 μmol/L. Similarly, the proportion of apoptotic cells was significantly increased from 7.27% to 39.36% after 48 h treatment (Fig. 5C), and clear cleavages of PARP and caspase-3 occurred when treated with 20μmol/L of nitidine chloride (Fig. 5D).

Nitidine chloride suppresses tumor angiogenesis and tumor growth in a human gastric cancer xenograft mouse model.

To evaluate the efficacy of nitidine chloride on tumor growth and tumor angiogenesis *in vivo*, we further transplanted SGC-7901 cells into mice and constructed human gastric cancer xenograft mouse model. We found that intra-peritoneal administration of nitidine chloride (7 mg/kg/d, 20 d) led to significant inhibition of tumor volume (Fig. 6A1) and tumor weight (Fig. 6A2, $P<0.001$), without noticeable toxicity (Fig. 6A3) as compared with the counterparts treated with DMSO. The average volume of solid tumors in nitidine chloride-treated mice (300.51±53.13 mm^3) was much smaller than that of control group (796.84±79.21 mm^3) (Fig. 6B1). Interestingly, when the skin of each mouse was pulled back to expose an intact tumor, we found that tumor growth suppression mediated by nitidine chloride was well correlated with angiogenesis inhibition (Fig. 6B2).

To examine the molecular target and neovascularization in solid tumors, we further performed immunohistochemistry with STAT3, CD31 and VEGF antibodies. As shown by Fig.6C, nitidine chloride dramatically reduced the expression of STAT3 and VEGF in solid tumors. The number of CD31-positive endothelial cells in the nitidine chloride-treated xenografts accordingly decreased. Both the levels of STAT3 phosphorylation and total STAT3 protein in randomly selected tumors of the two groups were also remarkably different, as showed by Western blotting results (Fig. 6D). Together, our findings demonstrated that nitidine chloride significantly suppressed both tumor growth and tumor angiogensis *in vivo* by interfering with STAT3 signaling pathway.

Discussion

More recently, increasing attention has been devoted to the aberrant activation of STAT3 for its critical role in tumor progression (33-35). However, therapeutic agents targeting STAT3 signaling pathway are still limited. In our present study, we clearly evaluated the anticancer potential of nitidine chloride *in vitro* and *in vivo,* and found, for the first time, that nitidine chloride effectively inhibited tumor angiogenesis and tumor growth of human gastric cancer by interfering with STAT3 signaling pathway.

Angiogenesis has been an attractive target for drug therapy due to its pivotal role in tumor growth and metastasis (4, 36), and anti-angiogenic therapy is now considered as the forth strategy to treat cancer (4, 37). Angiogenesis is a complex multi-step process that involves endothelial cell proliferation, migration and tube formation triggered by specific growth factors in tumor microenvironment. In this study, we found that nitidine chloride effectively abrogated VEGF-induced HUVECs proliferation, invasion and capillary-like structures formation *in vitro,* even at sub-lethal concentrations. In addition, VEGF-triggered neovascularization in the Matrigel plugs and in the mouse cornea *in vivo* were also dramatically suppressed by nitidine chloride, providing a critical clue to the ability of this alkaloid to inhibit angiogenesis. When compared the effective concentrations of nitidine chloride on endothelial cells (Fig.1, 5~10 μmol/L) and gastric epithelial cells (Fig.5, 20~30 μmol/L), we found that nitidine chloride's antiangiogenic activity may be much earlier than its cytotoxic effects on tumor cells.

Previous reports have shown a close association between STAT3 activation and gastric cancer growth and revascularization (38-39). Moreover, activation of STAT3 has been directly correlated with VEGF production (40). Our present investigation showed that both mRNA and protein

expression of VEGF were dose-dependently suppressed by nitidine chloride *via* STAT3 inhibition in human gastric cancer cells. VEGF was initially thought to mediate its signaling in a paracrine manner by acting on neighboring endothelial cells *via* VEGF receptor 2 (VEGFR2), which was specifically expressed on the endothelial-cell surface and believed to regulate the majority of the angiogenic effects of VEGF (23, 36, 41). In this study, we found that nitidine chloride dose-dependently inhibited the phophorylation of VEGFR2 (Tyr^{1175}) in HUVECs, which may lead to the inhibition of a number of downstream signaling cascades. STAT3 is principally activated by non-receptor tyrosine kinase JAK2 (42), and c-Src family kinase has also been involved in STAT3 phosphorylation (43). Our results showed that phophorylation of Src (Tyr^{416}), JAK1 ($Tyr^{1022/1023}$) and JAK2 ($Tyr^{1007/1008}$) was dose- and time-dependently blocked by nitidine chloride in endothelial cells (Fig.3), indicating that the direct effects of nitidine chloride on angiogenesis might be through inhibiting the VEGFR2/STAT3 signaling cascade. As evidenced by our previous reports, other natural compounds, such as indirubin (44) and cucurbitacin E (45), similarly inhibited tumor angiogenesis via blocking VEGFR2-mediated JAK2/STAT3 pathway.

As previously mentioned, STAT3 participates in tumorigenesis through up-regulation of genes encoding apoptosis inhibitors (Bcl-xL, Bcl-2 and survivin) and cell cycle regulators (Cyclin D1 and c-Myc) (46). In this study, we found that nitidine chloride blocked the activation STAT3 in SGC-7901 and AGS gastric cancer cells, indicating that the STAT3 suppressive activity of nitidine is not cell type-specific. Bcl-xL is an anti-apoptotic protein of the Bcl-2 family that inhibits apoptosis by preventing cytochrome c release (47). High level of Bcl-xL expression has been associated with advanced malignancies and poor prognosis (48). Therefore, suppression of Bcl-2 and Bcl-xL expression may be a useful strategy to potentiate cancer apoptosis (49-50). Notably, we found that

STAT3-dependent target genes including Bcl-2 and Bcl-xL were dose-dependently down-regulated by nitidine chloride. Constitutively active STAT3 has been implicated in the induction of resistance to apoptosis, possibly through the expression of Bcl-2, Bcl-xL, and Cyclin D1 (46). Our findings implied that suppression of STAT3 activation by nitidine chloride could facilitate cancer cell apoptosis. In agreement with this assumption, nitidine-treated SGC-7901 gastric cancer cells undergo clear death and apoptosis, as indicated by increased cleavage of caspase-3 and PARP in cytoplasm (Fig. 5). Additionally, proliferative (Cyclin D1), antiapopotic (Bcl-2, Bcl-xL) and proangiogenic genes (VEGF) of STAT3 were all down-regulated by nitidine's treatment, suggesting a positive feedback loop and a close association between nitidine chloride-mediated inhibition on angiogenesis and tumor growth. However, further studies are needed to carefully substantiate this speculation.

To evaluate the anti-tumor activity of nitidine chloride *in vivo*, athymic nude mice were transplanted with human gastric cancer cells and treated with nitidine chloride. We found that nitidine chloride significantly suppressed the growth of gastric tumor xenografts (the inhibition rate of 65% at dosage of 7 mg/kg/d) and also dramatically reduced neovascularization. Considering the effective antiangiogenesis of nitidine chloride in the Matrigel plugs and mouse cornea, we deem that nitidine chloride inhibits tumor growth *in vivo,* not only directly inhibiting tumor cell proliferation but also through suppression of tumor angiogenesis. We further clearly demonstrated a reduced expression of VEGF and STAT3 protein in the tumors of nitidine-treated mice as compared to the tumors of DMSO-treated mice. Taken together, our findings is the first to provide convincing evidence that nitidine chloride suppresses gastric tumor growth and tumor angiogenesis by suppressing constitutively activated STAT3 signaling cascade, making the compound a promising agent for the treatment of cancer and angiogenesis-related pathologies. However, further studies are

needed to carefully substantiate this speculation on the precise target of nitidine chloride in coordinately suppression of angiogenesis and tumor growth.

References

1. Jemal A, Bray F, Center MM, Ferlay J, Ward E, Forman D. Global cancer statistics. CA Cancer J Clin. 2011;61:69-90.

2. Jemal A, Siegel R, Ward E, Hao Y, Xu J, Thun MJ. Cancer statistics, 2009. CA Cancer J Clin. 2009;59:225-49.

3. Kitadai Y. Angiogenesis and lymphangiogenesis of gastric cancer. J Oncol. 2010;2010:468725.

4. Cook KM, Figg WD. Angiogenesis inhibitors: current strategies and future prospects. CA Cancer J Clin. 2010;60:222-43.

5. Yang S, Ngo VC, Lew GB, Chong LW, Lee SS, Ong WJ, et al. AZD6244 (ARRY-142886) enhances the therapeutic efficacy of sorafenib in mouse models of gastric cancer. Mol Cancer Ther. 2009;8:2537-45.

6. Xu Q, Briggs J, Park S, Niu G, Kortylewski M, Zhang S, et al. Targeting Stat3 blocks both HIF-1 and VEGF expression induced by multiple oncogenic growth signaling pathways. Oncogene. 2005;24:5552-60.

7. Jung JE, Lee HG, Cho IH, Chung DH, Yoon SH, Yang YM, et al. STAT3 is a potential modulator of HIF-1-mediated VEGF expression in human renal carcinoma cells. FASEB J. 2005;19:1296-8.

8. Buettner R, Mora LB, Jove R. Activated STAT signaling in human tumors provides novel molecular targets for therapeutic intervention. Clin Cancer Res. 2002;8:945-54.

9. Diaz N, Minton S, Cox C, Bowman T, Gritsko T, Garcia R, et al. Activation of stat3 in primary tumors from high-risk breast cancer patients is associated with elevated levels of activated SRC and survivin expression. Clin Cancer Res. 2006;12:20-8.

10. Gamero AM, Young HA, Wiltrout RH. Inactivation of Stat3 in tumor cells: releasing a brake on

immune responses against cancer? Cancer Cell. 2004;5:111-2.

11. Yu ZY, Huang R, Xiao H, Sun WF, Shan YJ, Wang B, et al. Fluacrypyrim, a novel STAT3 activation inhibitor, induces cell cycle arrest and apoptosis in cancer cells harboring constitutively-active STAT3. Int J Cancer. 2010;127:1259-70.

12. Pathak AK, Bhutani M, Nair AS, Ahn KS, Chakraborty A, Kadara H, et al. Ursolic acid inhibits STAT3 activation pathway leading to suppression of proliferation and chemosensitization of human multiple myeloma cells. Mol Cancer Res. 2007;5:943-55.

13. Heath VL, Bicknell R. Anticancer strategies involving the vasculature. Nat Rev Clin Oncol. 2009;6:395-404.

14. Newman DJ, Cragg GM, Snader KM. Natural products as sources of new drugs over the period 1981-2002. J Nat Prod. 2003;66:1022-37.

15. Hu J, Zhang WD, Liu RH, Zhang C, Shen YH, Li HL, et al. Benzophenanthridine alkaloids from Zanthoxylum nitidum (Roxb.) DC, and their analgesic and anti-inflammatory activities. Chem Biodivers. 2006;3:990-5.

16. Iwasaki H, Okabe T, Takara K, Toda T, Shimatani M, Oku H. Tumor-selective cytotoxicity of benzo[c]phenanthridine derivatives from Toddalia asiatica Lam. Cancer Chemother Pharmacol. 2010;65:719-26.

17. Xu Q, Li ZX, Ye ZM. [Nitidine chloride-induced apoptosis of human osteosarcoma cells and its mechanism]. Nan Fang Yi Ke Da Xue Xue Bao. 2011;31:361-4.

18. van Dross RT, Sanders MM. Molecular characterization of recombinant Pneumocystis carinii topoisomerase I: differential interactions with human topoisomerase I poisons and pentamidine. Antimicrob Agents Chemother. 2002;46:2145-54.

19. Tan GT, Pezzuto JM, Kinghorn AD, Hughes SH. Evaluation of natural products as inhibitors of human immunodeficiency virus type 1 (HIV-1) reverse transcriptase. J Nat Prod. 1991;54:143-54.

20. Moser C, Lang SA, Mori A, Hellerbrand C, Schlitt HJ, Geissler EK, et al. ENMD-1198, a novel tubulin-binding agent reduces HIF-1alpha and STAT3 activity in human hepatocellular carcinoma(HCC) cells, and inhibits growth and vascularization in vivo. BMC Cancer. 2008;8:206.

21. Jung JE, Kim HS, Lee CS, Park DH, Kim YN, Lee MJ, et al. Caffeic acid and its synthetic derivative CADPE suppress tumor angiogenesis by blocking STAT3-mediated VEGF expression in human renal carcinoma cells. Carcinogenesis. 2007;28:1780-7.

22. Pang X, Yi T, Yi Z, Cho SG, Qu W, Pinkaew D, et al. Morelloflavone, a biflavonoid, inhibits tumor angiogenesis by targeting rho GTPases and extracellular signal-regulated kinase signaling pathways. Cancer Res. 2009;69:518-25.

23. Pang X, Yi Z, Zhang X, Sung B, Qu W, Lian X, et al. Acetyl-11-keto-beta-boswellic acid inhibits prostate tumor growth by suppressing vascular endothelial growth factor receptor 2-mediated angiogenesis. Cancer Res. 2009;69:5893-900.

24. Pyun BJ, Choi S, Lee Y, Kim TW, Min JK, Kim Y, et al. Capsiate, a nonpungent capsaicin-like compound, inhibits angiogenesis and vascular permeability via a direct inhibition of Src kinase activity. Cancer Res. 2008;68:227-35.

25. Ziche M, Morbidelli L. The corneal pocket assay. Methods Mol Biol. 2009;467:319-29.

26. Takada Y, Gillenwater A, Ichikawa H, Aggarwal BB. Suberoylanilide hydroxamic acid potentiates apoptosis, inhibits invasion, and abolishes osteoclastogenesis by suppressing nuclear factor-kappaB activation. J Biol Chem. 2006;281:5612-22.

27. Bharti AC, Donato N, Aggarwal BB. Curcumin (diferuloylmethane) inhibits constitutive and

IL-6-inducible STAT3 phosphorylation in human multiple myeloma cells. J Immunol. 2003;171:3863-71.

28. Yu CL, Meyer DJ, Campbell GS, Larner AC, Carter-Su C, Schwartz J, et al. Enhanced DNA-binding activity of a Stat3-related protein in cells transformed by the Src oncoprotein. Science. 1995;269:81-3.

29. Ye SK, Agata Y, Lee HC, Kurooka H, Kitamura T, Shimizu A, et al. The IL-7 receptor controls the accessibility of the TCRgamma locus by Stat5 and histone acetylation. Immunity. 2001;15:813-23.

30. Pang X, Yi Z, Zhang J, Lu B, Sung B, Qu W, et al. Celastrol suppresses angiogenesis-mediated tumor growth through inhibition of AKT/mammalian target of rapamycin pathway. Cancer Res. 2010;70:1951-9.

31. Kim DY, Cha ST, Ahn DH, Kang HY, Kwon CI, Ko KH, et al. STAT3 expression in gastric cancer indicates a poor prognosis. J Gastroenterol Hepatol. 2009;24:646-51.

32. Jackson CB, Giraud AS. STAT3 as a prognostic marker in human gastric cancer. J Gastroenterol Hepatol. 2009;24:505-7.

33. Yang C, Schwab JH, Schoenfeld AJ, Hornicek FJ, Wood KB, Nielsen GP, et al. A novel target for treatment of chordoma: signal transducers and activators of transcription 3. Mol Cancer Ther. 2009;8:2597-605.

34. Lee HJ, Seo NJ, Jeong SJ, Park Y, Jung DB, Koh W, et al. Oral administration of Penta-O-galloyl-{beta}-D-glucose Suppresses Triple-negative Breast Cancer Xenograft Growth and Metastasis in Strong Association with JAK1-STAT3 Inhibition. Carcinogenesis. 2011.

35. Pandey MK, Sung B, Aggarwal BB. Betulinic acid suppresses STAT3 activation pathway

through induction of protein tyrosine phosphatase SHP-1 in human multiple myeloma cells. Int J Cancer. 2010;127:282-92.

36. Kerbel RS. Tumor angiogenesis. N Engl J Med. 2008;358:2039-49.

37. Reinacher-Schick A, Pohl M, Schmiegel W. Drug insight: antiangiogenic therapies for gastrointestinal cancers--focus on monoclonal antibodies. Nat Clin Pract Gastroenterol Hepatol. 2008;5:250-67.

38. Zhu BH, Chen HY, Zhan WH, Wang CY, Cai SR, Wang Z, et al. (-)-Epigallocatechin-3-gallate inhibits VEGF expression induced by IL-6 via Stat3 in gastric cancer. World J Gastroenterol. 2011;17:2315-25.

39. Zhu BH, Zhan WH, Li ZR, Wang Z, He YL, Peng JS, et al. (-)-Epigallocatechin-3-gallate inhibits growth of gastric cancer by reducing VEGF production and angiogenesis. World J Gastroenterol. 2007;13:1162-9.

40. Chen Z, Han ZC. STAT3: a critical transcription activator in angiogenesis. Med Res Rev. 2008;28:185-200.

41. Meng Y, Tang W, Dai Y, Wu X, Liu M, Ji Q, et al. Natural BH3 mimetic (-)-gossypol chemosensitizes human prostate cancer via Bcl-xL inhibition accompanied by increase of Puma and Noxa. Mol Cancer Ther. 2008;7:2192-202.

42. Ren Z, Schaefer TS. ErbB-2 activates Stat3 alpha in a Src- and JAK2-dependent manner. J Biol Chem. 2002;277:38486-93.

43. Schreiner SJ, Schiavone AP, Smithgall TE. Activation of STAT3 by the Src family kinase Hck requires a functional SH3 domain. J Biol Chem. 2002;277:45680-7.

44. Zhang X, Song Y, Wu Y, Dong Y, Lai L, Zhang J, et al. Indirubin inhibits tumor growth by

anti-tumor angiogenesis through blocking VEGFR2 mediated JAK/STAT3 signaling in endothelial cell. Int J Cancer. 2011.

45. Dong Y, Lu B, Zhang X, Zhang J, Lai L, Li D, et al. Cucurbitacin E, a tetracyclic triterpenes compound from Chinese medicine, inhibits tumor angiogenesis through VEGFR2-mediated Jak2-STAT3 signaling pathway. Carcinogenesis. 2010;31:2097-104.

46. Darnell JE, Jr. Transcription factors as targets for cancer therapy. Nat Rev Cancer. 2002;2:740-9.

47. Finucane DM, Bossy-Wetzel E, Waterhouse NJ, Cotter TG, Green DR. Bax-induced caspase activation and apoptosis via cytochrome c release from mitochondria is inhibitable by Bcl-xL. J Biol Chem. 1999;274:2225-33.

48. Linjawi A, Kontogiannea M, Halwani F, Edwardes M, Meterissian S. Prognostic significance of p53, bcl-2, and Bax expression in early breast cancer. J Am Coll Surg. 2004;198:83-90.

49. Varin E, Denoyelle C, Brotin E, Meryet-Figuiere M, Giffard F, Abeilard E, et al. Downregulation of Bcl-xL and Mcl-1 is sufficient to induce cell death in mesothelioma cells highly refractory to conventional chemotherapy. Carcinogenesis. 2010;31:984-93.

50. Brotin E, Meryet-Figuiere M, Simonin K, Duval RE, Villedieu M, Leroy-Dudal J, et al. Bcl-XL and MCL-1 constitute pertinent targets in ovarian carcinoma and their concomitant inhibition is sufficient to induce apoptosis. Int J Cancer. 2010;126:885-95.

Figure legends

Figure 1. Nitidine chloride inhibits VEGF-induced endothelial cell proliferation, migration and tubular-structures formation *in vitro*. *A*, the chemical structure of nitidine chloride. *B*, Nitidine chloride significantly inhibited cell proliferation dose-dependently. Cell viability was determined by MTS assay. *C*, nitidine chloride remarkably inhibited VEGF-induced endothelial cells migration. *D*, nitidine chloride remarkably inhibited the tube formation of endothelial cells. *Columns*, mean from three independent experiments with triplicate; *bars*, standard deviation; **, $P < 0.01$ *vs.* VEGF alone group.

Figure 2. Nitidine chloride inhibits VEGF-induced angiogenesis *in vivo*. *A*, representative images of Matrigel plugs in each group (n=4~6). *B*, immunohistochemistry analysis with CD31 antibody was performed on the sections of Matrigel plugs (magnification, 400×), showing CD31-positive endothelial cells. *C*, representative images of neovascularization in mouse corneal assay. *Columns*, mean from two independent experiments; *bars*, standard deviation; **, $P < 0.01$ *vs.* VEGF alone group.

Figure 3. Nitidine chloride inhibits STAT3 cascade in endothelial cells. *A*, nitidine chloride suppressed the activation of VEGFR2 (Tyr^{1175}) triggered by VEGF in endothelial cell by Western blotting analysis. *B*, nitidine chloride diminished the activation of STAT3, JAK1, JAK2, and Src kinase in a dose- and time-dependent manner in HUVECs. *C*, nitidine chloride dose-dependently inhibited VEGF-induced DNA binding activity of STAT3 in endothelial cells. Nuclear extract was prepared and examined by EMSA assay. Three independent experiments were performed.

Figure 4. Nitidine chloride blocks STAT3 signaling and suppresses STAT3 transcriptional activity in gastric cancer cells. *A*, nitidine chloride concentration- and time-dependently inhibited the activation of STAT3 in gastric tumor cells by Western blotting analysis. *B*, nitidine chloride inhibits STAT3 DNA-binding in a dose-dependent manner in SGC-7901 cells analyzed by EMSA assay. *C*, nitidine chloride suppressed the expression of both mRNA (left) and protein (right) of Bcl-2, Bcl-xL, Cyclin D1, and VEGF in SGC-7901 cells. *D*, nitidine chloride inhibited STAT3-dependent transcriptional activity of Bcl-xL (*D1*), Cyclin D1 (*D2*), and VEGF (*D3*) by ChIP assay. Beta-actin and GAPDH were used as internal controls. Three independent experiments were performed.

Figure 5. Nitidine chloride induces apoptosis of gastric cancer cell lines in a dose-dependent manner. *A*, nitidine chloride significantly suppressed viability of several gastric cancer cell lines measured by MTS assay. *B*, treatment of nitidine chloride destroyed plasma membrane integrity of SGC-7901 cells, as indicated by live-dead staining. *C*, nitidine chloride-mediated cell apoptosis were detected by flow cytometry assay. *D*, nitidine chloride dose-dependently induced cleavage of caspase-3 and PARP in cancer cells. Similar results were obtained in three independent experiments.

Figure 6. Nitidine chloride suppresses tumor growth and angiogenesis in a human gastric cancer xenograft mouse model. *A*, nitidine chloride inhibited tumor growth as measured by tumor volume (*left*) and tumor weight (*middle*) without detectable toxicity (*right*) at the tested dose. *Columns and dots*, mean; *bars*, standard deviation; ***, $P<0.001$ *vs.* the control group. *B*, nitidine

chloride inhibits both solid tumors (*B1*) and neovascularization (*B2*). *C,* immunohistochemical staining results of STAT3, VEGF and CD31 on tumor sections (magnification, 400×). *D,* nitidine chloride dramatically suppressed activation of p-STAT3 and total STAT3 expression in solid tumors. Three random tumors were selected in two groups and corresponding protein was applied to Western blotting analysis.

Figure 1

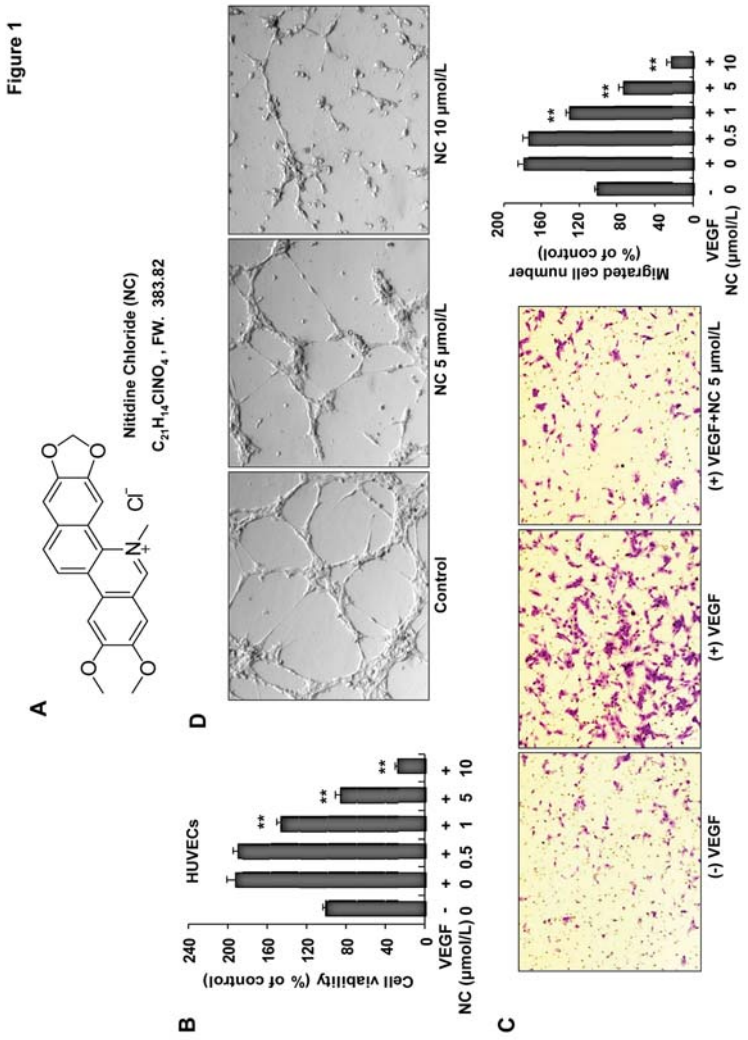

Figure 2

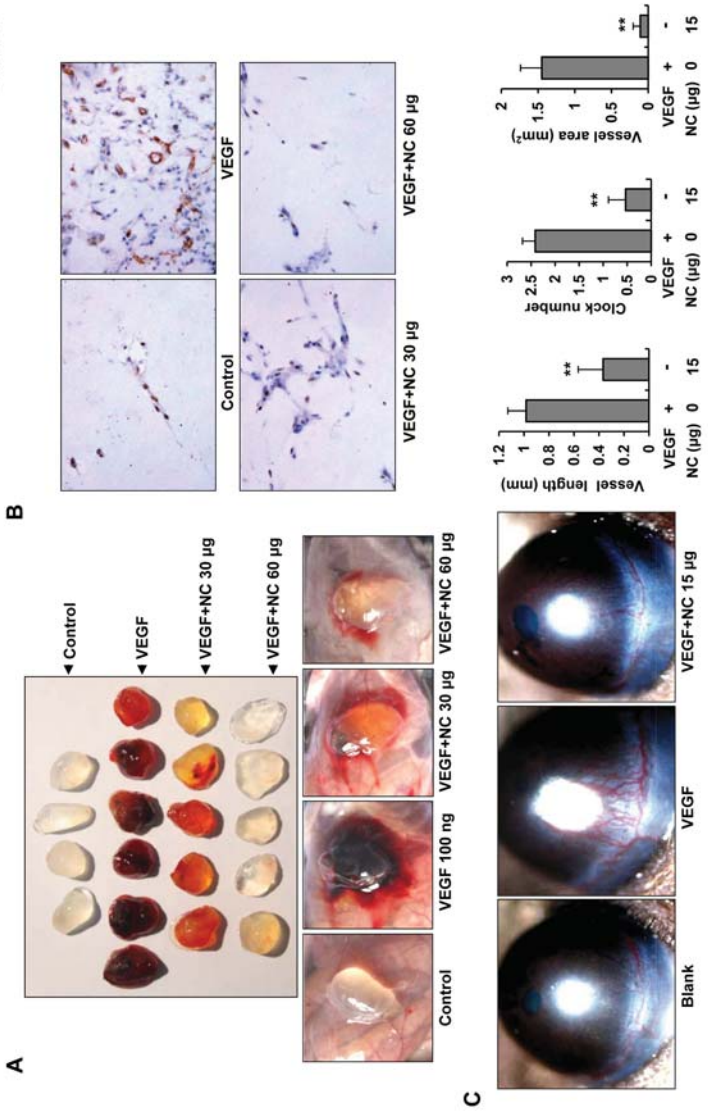

Figure 3

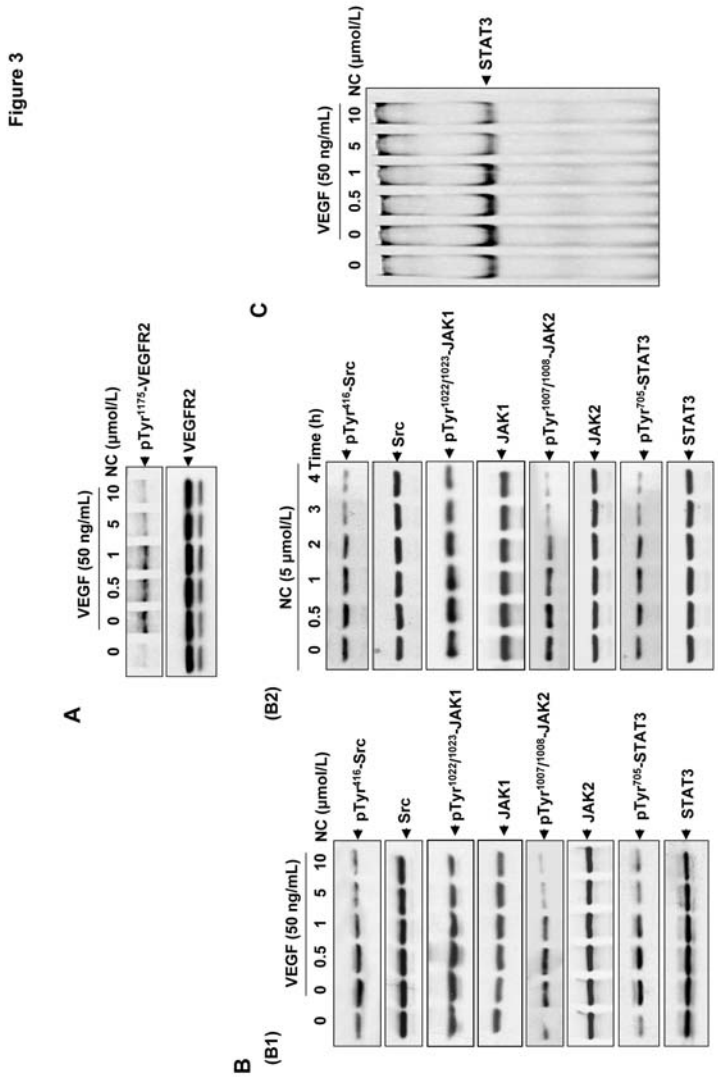

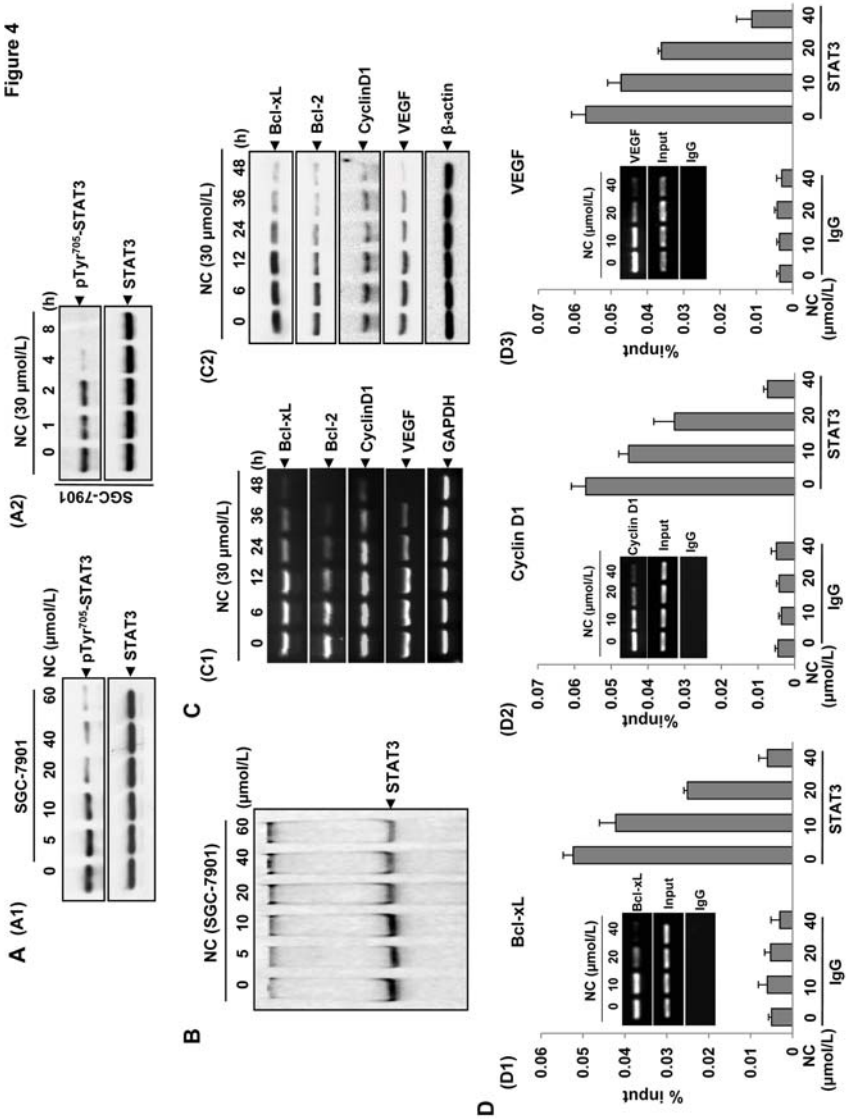

Author Manuscript Published OnlineFirst on December 27, 2011; DOI: 10.1158/1535-7163.MCT-11-0648
Author manuscripts have been peer reviewed and accepted for publication but have not yet been edited.

Figure 5

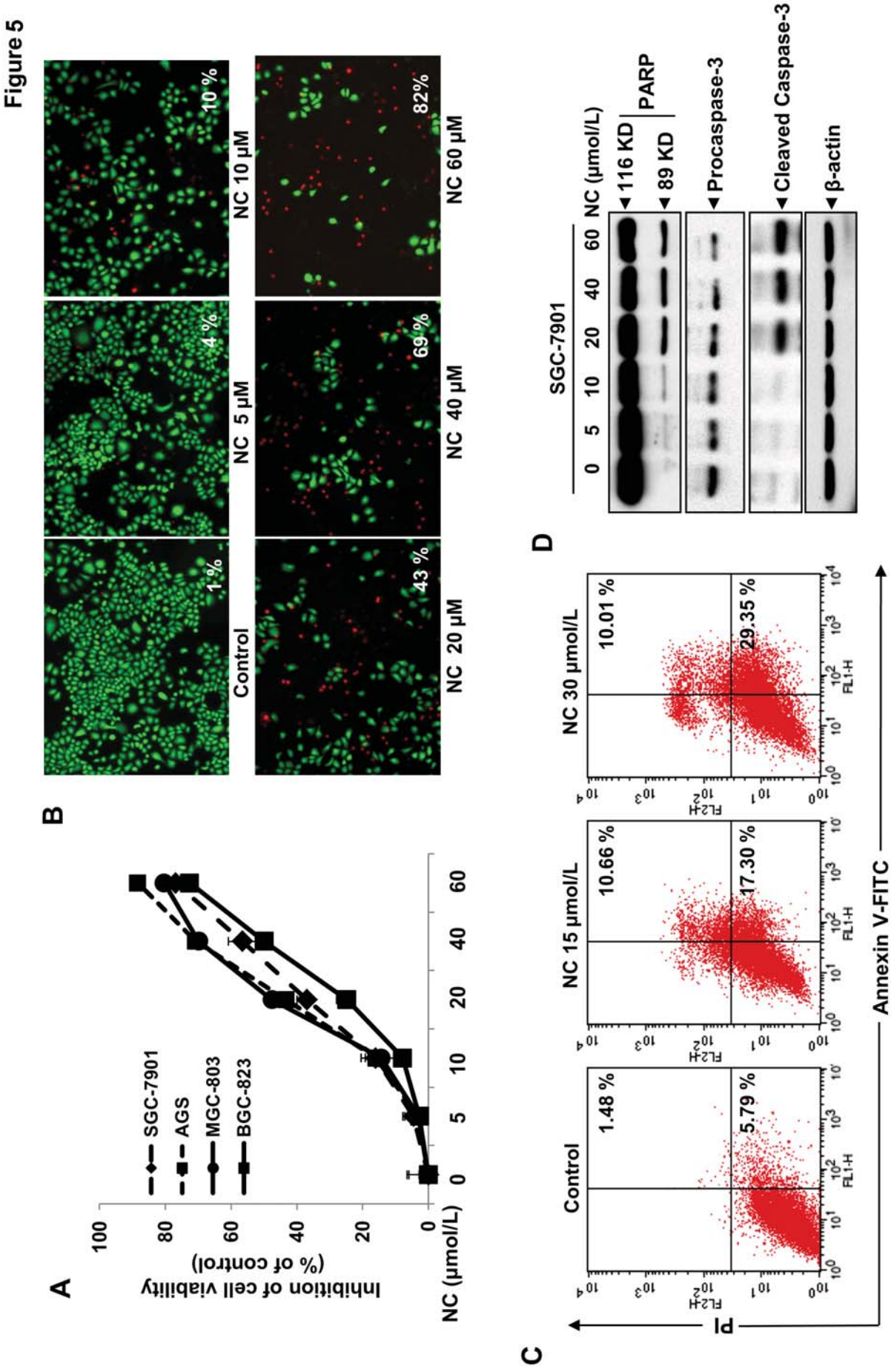

Author Manuscript Published OnlineFirst on December 27, 2011; DOI: 10.1158/1535-7163.MCT-11-0648
Author manuscripts have been peer reviewed and accepted for publication but have not yet been edited.

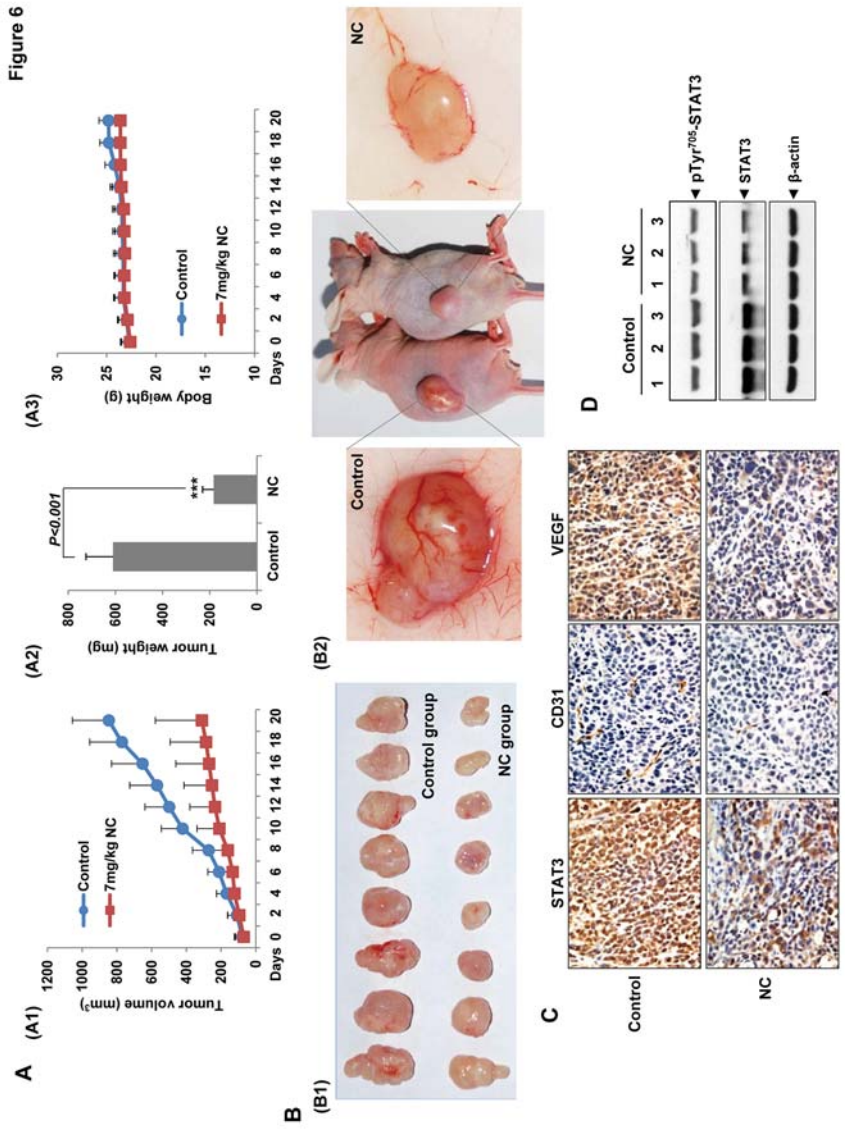

AACR American Association for Cancer Research

Molecular Cancer Therapeutics

Inhibition of STAT3 Signaling Pathway by Nitidine Chloride Suppressed the Angiogenesis and Growth of Human Gastric Cancer

Jing Chen, Jieqiong Wang, Lei Lin, et al.

Mol Cancer Ther Published OnlineFirst December 27, 2011.